Supplementary Materials: Tumor priming by SMO inhibitor enhances anti-EGFR antibody delivery and efficacy in a pancreatic ductal adenocarcinoma model

Jun Wang [1], Darren K.W. Chan [1], Arindam Sen [2,3], Wen Wee Ma [4,†], Robert M. Straubinger [1,3,5,*]

Author Affiliations
[1] Department of Pharmaceutical Sciences and [2] Physiology and Biophysics, University at Buffalo, State University of New York, Buffalo, New York
Departments of [3] Cell Stress Biochemistry and Biophysics, [4] Medicine and [5] Pharmacology and Therapeutics, Roswell Park Comprehensive Cancer Center, Buffalo, New York

[*] **Corresponding Author:**
Department of Pharmaceutical Sciences
University at Buffalo, State University of New York
Buffalo, New York 14214
(716) 645-2844
rms@buffalo.edu

[†] **Current Address:**
Department of Medical Oncology, Mayo Clinic, Rochester, Minnesota 55905

Supplementary Materials and Methods

Quantification of cetuximab by ELISA

A sandwich ELISA method was developed to quantify cetuximab concentrations in plasma. Briefly, 96 well ELISA plates were coated with 100 µL of a 1:1000 dilution of rabbit monoclonal H26-10 anti-human IgG1 (ab125912, Abcam, Cambridge MA) in carbonate buffer, pH 9.5 at 4^{o}C overnight. The plates were blocked with 300 µL of 2% bovine serum albumin in Dulbecco's phosphate buffered saline (PBS), pH 7.2 for 2 h, and a 100 µL plasma sample was incubated in each well at 4^{o}C overnight. After washing with PBS, 100 µL of a 1:20,000 dilution of goat anti-human polyclonal antibody conjugated with biotin (Ab7152, Abcam) was added to each well and the plates were incubated at room temperature for 2 h. Plates were washed with PBS containing 0.05% Tween 20, and then incubated with 100 µL of a 1:20,000 dilution of HRP-conjugated streptavidin (ab7403, Abcam) at room temperature for 1 h. After washing, 100 µL of substrate solution (TMB microwell peroxidase substrate system, 50-76-11, KPL, Inc. , Gaithersburg, MD) was added to each well for 30 minutes, and the reaction was stopped with 1 M phosphoric acid. Absorbance at 450 nm was measured. The ELISA assay was validated each time using a cetuximab standard concentration curve.

Fluorescent nanoparticles as probes of tumor permeability

Sterically-stabilized liposomes (SSL) of 80-100 nm were prepared as probes of tumor vascular barrier compromise, as described previously (1). They were composed of 9:5:1 mol:mol:mol distearoylphosphatidylcholine:cholesterol:polyethyleneglycol-derivatized phosphatidylethanolamine (Avanti Polar Lipids, Alabaster AL) and contained 1 mol% of the nonexchangeable dialkyl carbocyanine membrane label DiIC18(5)-DS (SSL-DiI) (2,3) (Invitrogen, Carlsbad, CA), and were prepared by hydration of a thin lipid film with buffered saline and then extrusion through polycarbonate filters of decreasing pore diameter down to 80 nm. Mice were implanted from donor animals with patient-derived xenograft (PDX) pancreatic ductal adenocarcinomas (PDAC) selected from a 30-tumor panel (4). When tumors were approx. 300 mm^3 in volume, the mice were randomized into groups. To initiate tumor priming, the SMO inhibitor of sonic hedgehog signaling (sHHI) NVP-LDE225 (Novartis) was administered orally to groups of mice at 40 mg/kg/day. On days 0, 4, 7, and 10 of sHHI administration, SSL-DiI were administered *i.v.* 1 h after the sHHI dose, and mice were sacrificed 24 h later, at the peak time of SSL deposition. The tumors were harvested and bisected. Half was embedded in OCT mounting medium (Tissue-tek, Sakura Finetek, Torrance, CA), flash-frozen, and 10 µm frozen sections were prepared and mounted with DAPI staining. Images of sections were acquired under uniform imaging conditions using a 20x objective lens on a Zeiss AxioImager fluorescence microscope (Thornwood, NY) and stitched into panoramas encompassing the entire tumor using Zeiss Zen image processing software.

Pharmacokinetic modeling of cetuximab plasma concentrations

Based on published literature and our data, the dose of cetuximab employed in these experiments was estimated to be sufficient to saturate all Epidermal Growth Factor receptors (EGFR) in the PDX model. Using this assumption, cetuximab plasma concentration data were fit with mathematical equations derived from a standard two compartment pharmacokinetic model with an i.v. bolus input. The parameter values were estimated by model fitting using Phoenix software (Certara Inc., Princeton, NJ). The plasma concentrations of cetuximab resulting from the dosing regimen used in the investigation of tumor growth inhibition (see parent manuscript) were then predicted by simulating multiple doses with the two compartment model.

Table S1. Mutation profiles of PDAC PDX models.

Tumor#	**Gender**	**Diagnosis**	**Genomic profiling results** *Gene, mutation, (mean copy #) call*
PANC-12424	Male	IPAI*	APC N22D, Y935X (1.33) Loss; BRCA2 D1420Y; CDKN2A (0.01) Loss; KRAS wt**; MAP2K1 K57T; PIK3R1 (1.29) Loss; TP53 R306X
PANC-14312	Male	IPAI	APC W157C (1.34) Loss; CDKN2A Y44X (0.97) Loss; KRAS G12R; MED12 S63N; PIK3CA M1040T; PIK3R1 A159QfsX18 (1.30) Loss; SMAD4 (0.77) Loss; TP53 R175H
PANC-18254	Female	IPAI	BRCA1 R841W; CDKN2A (0.01) Loss; GNAS R201H; KRAS G12V; MED12 S63N; NOTCH1 (1.37) Loss; PIK3CA M1040T; PIK3R1 A159Q; PTCH1 (1.07) Loss; PTEN (1.17) Loss; SMAD4 (0.01) Loss; TP53 (1.23) Loss; TSC1 (0.98) Loss
PANC-18269	Male	IPAI	APC E1317Q; BAP1 (1.09) Loss; BRAF S467L; BRCA2 I332F; CDKN2A (0.01) Loss; KRAS G12D; SMAD4 (1.14) Loss

*IPAI: Intraductal papillary adenocarcinoma with invasion
**wild type (no mutation of significance)

Tumor DNA sequencing for driver mutation analysis was performed by Omniseq, Inc. (Buffalo, NY) and the data have been deposited in the Sequence Read Archive of the National Center for Biotechnology Information, U.S. National Library of Medicine as BioProject Accession #PRJNA554899 https://www.ncbi.nlm.nih.gov/bioproject/PRJNA554899.

Table S2. Cetuximab pharmacokinetic parameter estimates in PDX-bearing mice model following a single i.v. bolus.

	Vehicle Treatment		NVP-LDE225	
	Estimated	**CV%**	**Estimated**	**CV%**
V1 (ml/kg)	77.8	0.04	83.1	10.7
CL (ml/hour/kg)	1.47	10.2	1.69	10.9
V2 (ml/kg)	98.8	22.4	131	20.0
CLd (ml/hour/kg)	4.81	30.5	8.08	28.8
Vss (ml/kg)	177	12.7	214	12.4

V1, apparent volume of the central compartment; V2, apparent volume of peripheral compartment; CL, systemic clearance; CLd, distribution clearance; Vss estimated steady-state volume of distribution

Supplementary Figures and Legends

Figure S1. Histology and stromal elaboration of PDAC PDX models

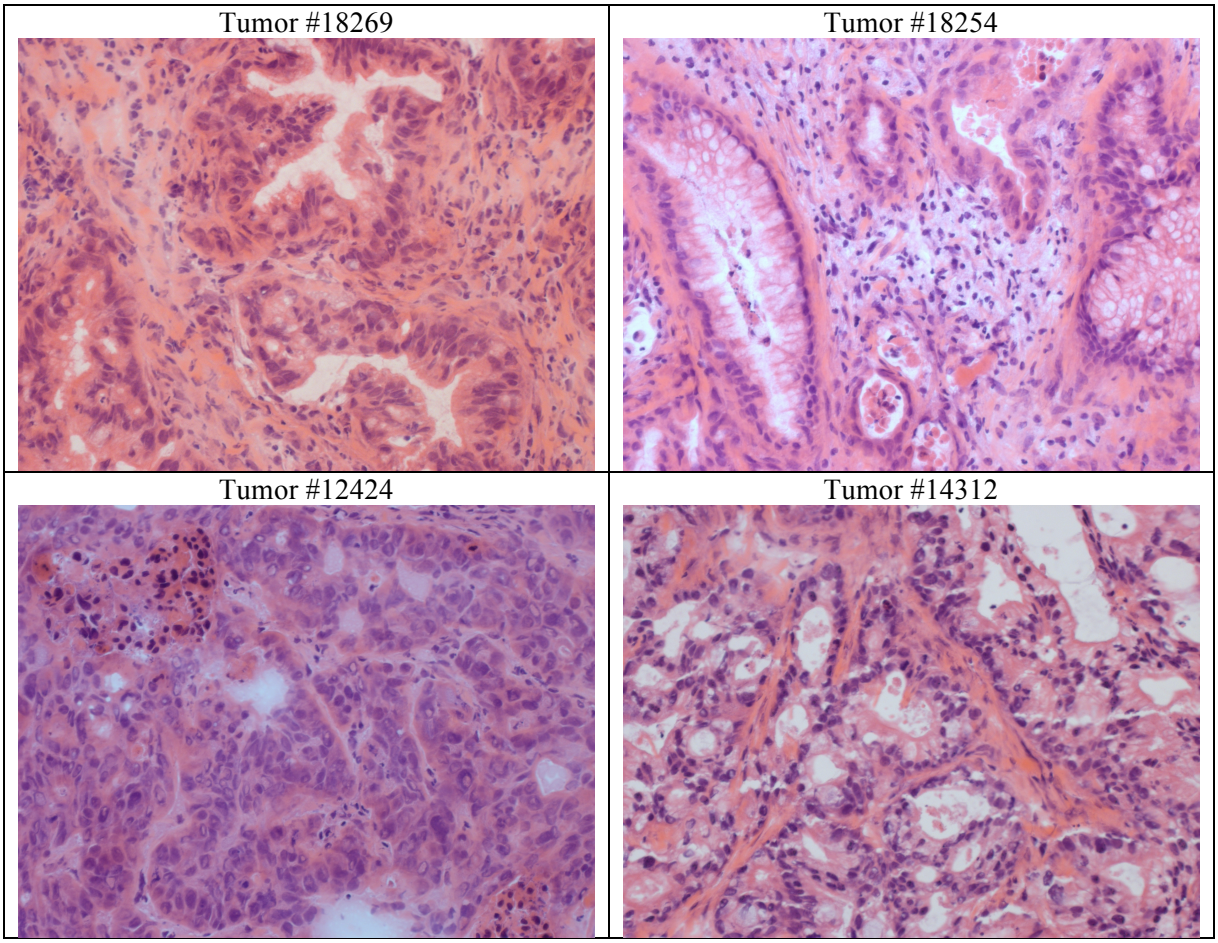

Representative H&E stained sections of PDAC PDX tumors employed in these studies, showing variable low-to-extensive desmoplasia with moderately- to poorly-differentiated adenocarcinoma cells lining glandular structures of differing abundance.

Figure S2. Effects of sHHI on tumor- vs. stromal GLI1 gene expression

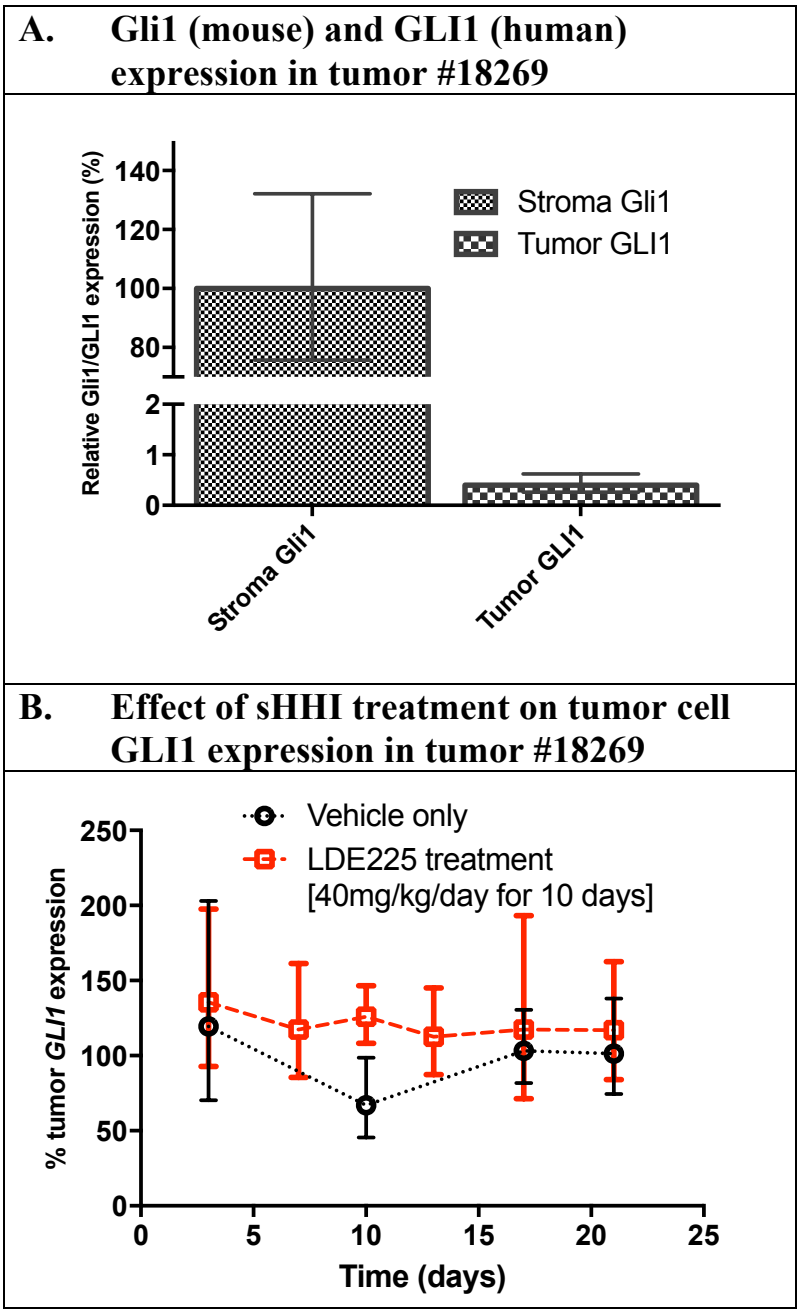

Human- and mouse-specific TaqMan primers (Applied Biosystems, Waltham, MA) were used in a quantitative real time/polymerase chain reaction (qRT-PCR) assay to evaluate the effects of sHH inhibitor upon expression of transcription factor GLI1 (human) and Gli1 (mouse) by PDX tumor #18269. Tumor-bearing mice were dosed *p.o.* daily by gavage for 10 days with 40 mg/kg NVP-LDE225 and sacrificed at intervals. **A.** Comparison of expression of stromal Gli1 with tumor cell GLI1. Data are normalized to vehicle-treated controls. Note split axis and scale change. **B.** There was no statistically significant effect of daily sHHI treatment on human GLI1 expression in tumors compared to vehicle-only controls.

Figure S3. Effect of sHHI on stromal Gli1 gene expression in different xenograft tumor models

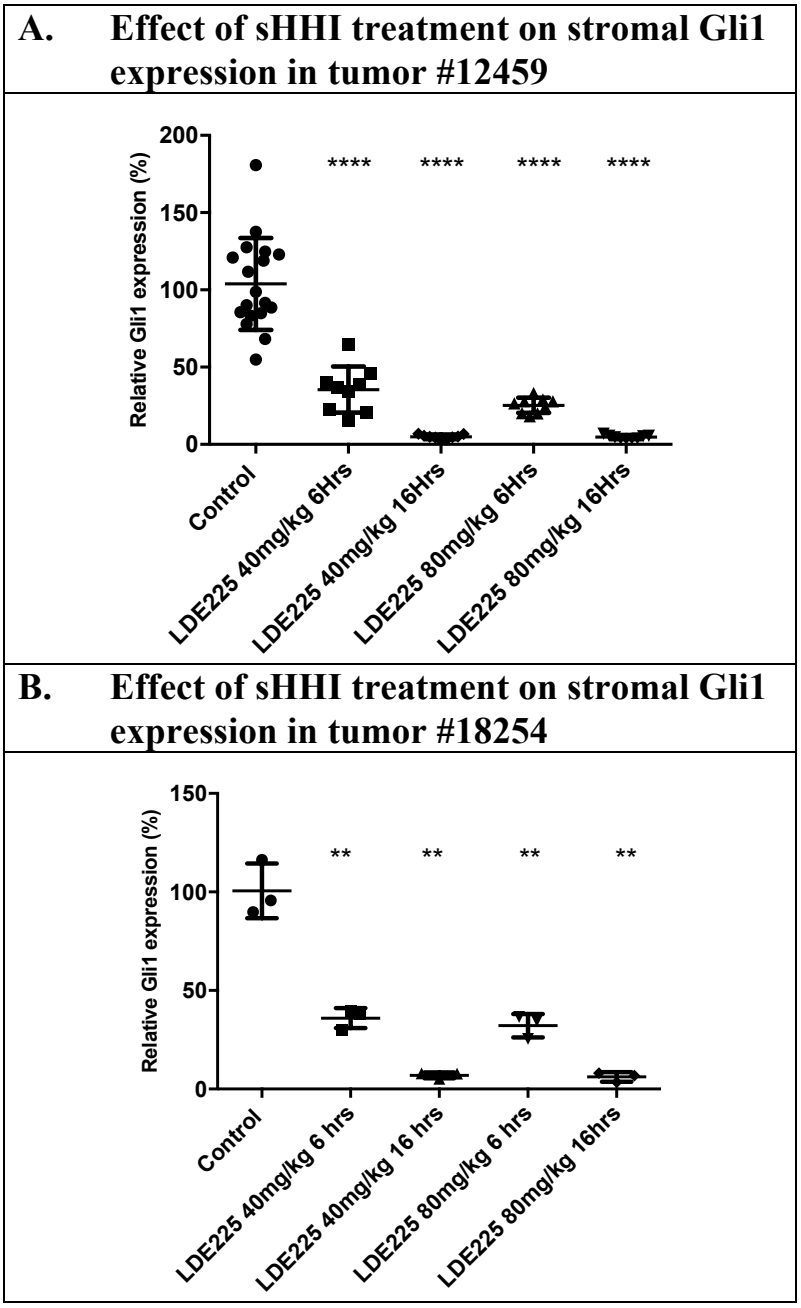

A qRT-PCR assay employing human- and mouse-specific TaqMan primers was used as in Figure S2 to evaluate the effects of the sHHI NVP-LDE225 upon tumor expression of transcription factor Gli1. Tumor-bearing mice were administered a single dose of 40 or 80 mg/kg LDE225 *p.o.* by gavage and sacrificed at intervals. Figure shows inhibition of stromal (mouse) Gli1 expression in (**A**) PDX tumor #12459 and (**B**) PDX tumor #18254. Statistical analysis was by unpaired t test with Welch's correction: ** $P < 0.01$; **** $P < 0.0001$).

Figure S4. Disposition of fluorescent nanoparticle probes in PDX tumors primed with sHH inhibitor treatment

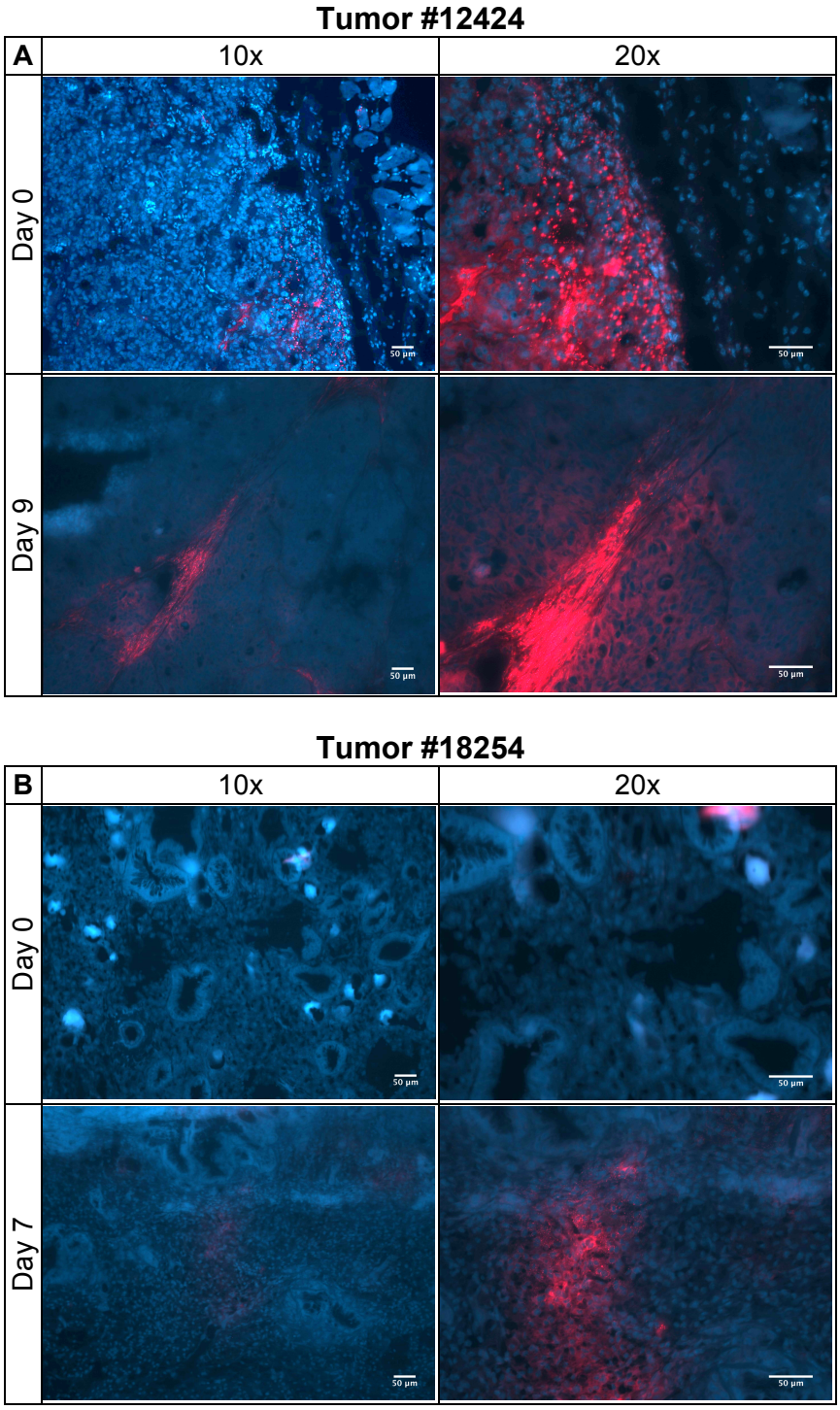

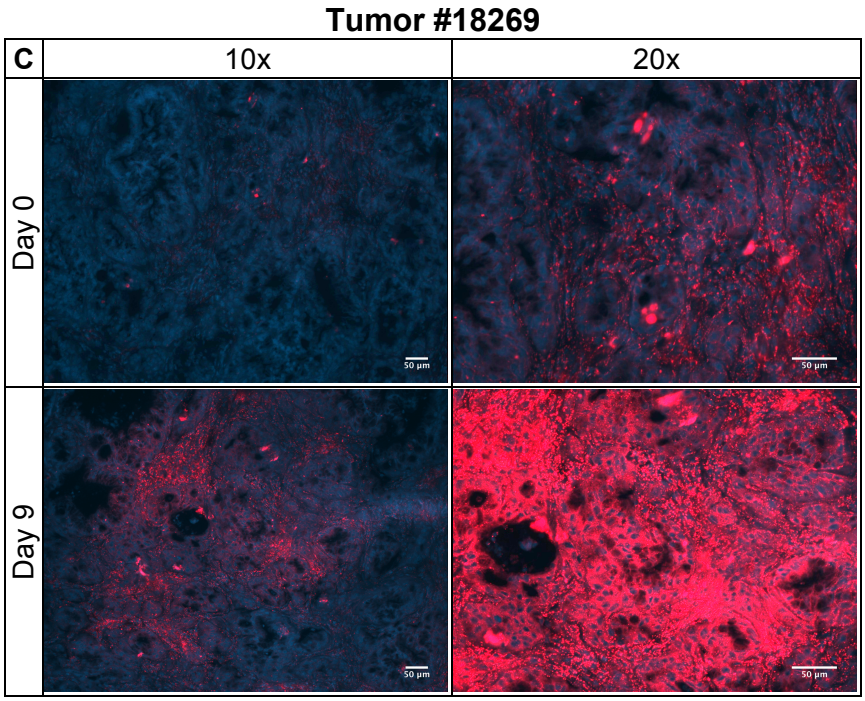

Mice bearing PDX tumors (**A**) #12424, (**B**) #18254, and (**C**) #18269, and (**D**) #14312 were treated with NVP-LDE225 (40mg/kg/day, *p.o.*) for up to 10 days. On various days, 80 nm fluorescent SSL-DiI were injected *i.v.* as a probe of tumor vascular permeability changes, and tumors were harvested 24 h later, at the peak time for tumor nanoparticle deposition. Images were acquired under similar imaging conditions using a Zeiss AxioImager fluorescence microscope at a range of magnifications. Red, liposomes; Blue, DAPI nuclear stain. Bar on each panel shows magnification. Most tumors showed peak nanoparticle deposition after approx. 7-9 days of sHHI treatment.

Figure S5. Effect of sHHI treatment on tumor vascular status

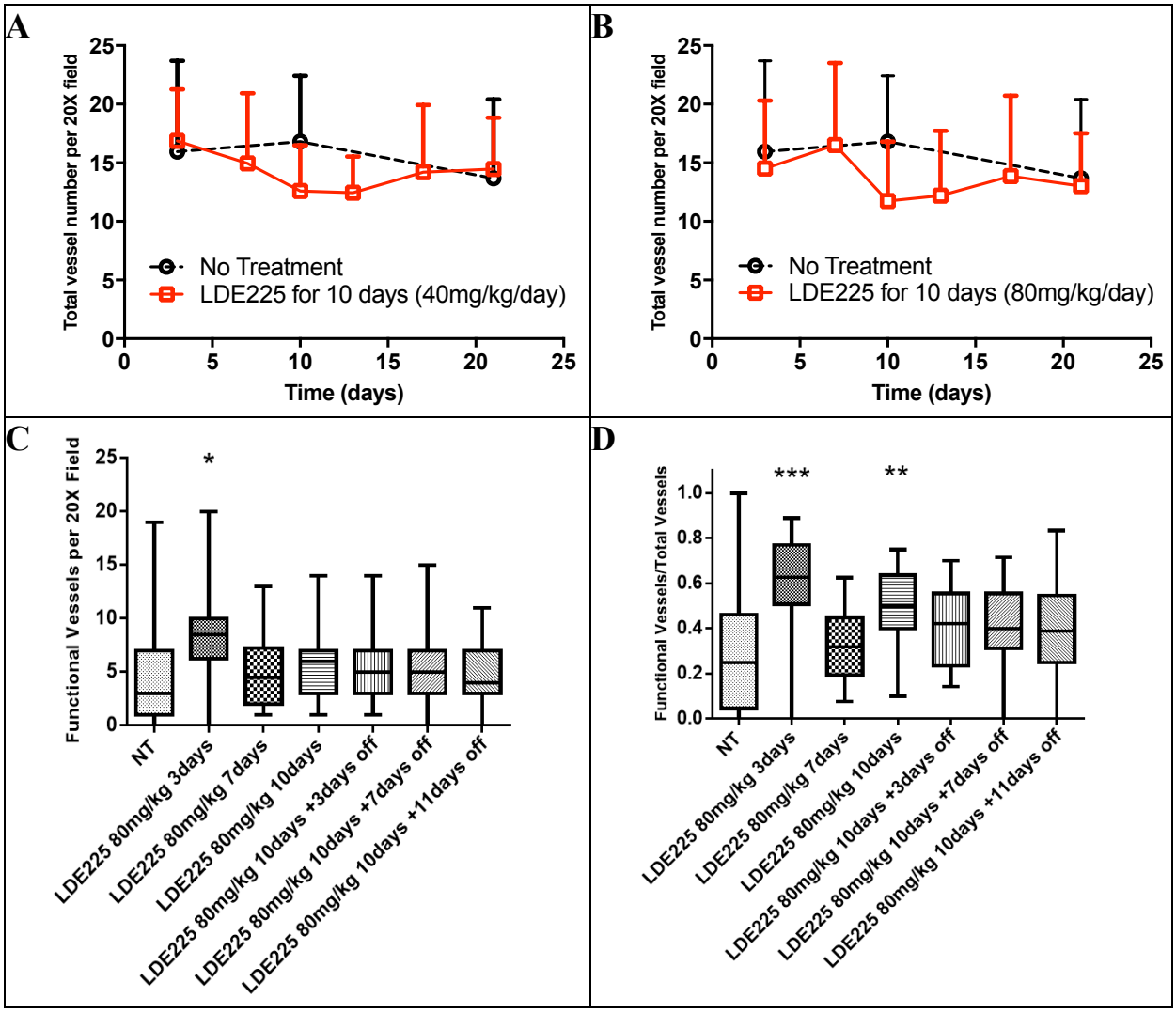

The effect of daily sHHI dosing upon total (A, B) and functional (C, D) microvessels was investigated. Mice bearing PDX #18269 tumors were dosed *p.o.* with 40 or 80 mg/kg/day NVP-LDE225 for up to 10 days, and tumors were sampled at intervals during and after the period of administration. CD31 was used as a marker for total microvessels, and functional microvessels were evaluated by injecting fluorescent *Lycopersicon esculentum* (*Le*) lectin *i.v.* 10 min before sacrifice. Three mice per treatment group were used, and a 20X objective was used to capture images of 5 random fields under uniform acquisition conditions for evaluation of *Le*-lectin fluorescence and $CD31^+$ staining. Average number of $CD31^+$ microvessels per field with (**A)** 40 or (**B**) 80 mg/kg/day NVP-LDE225 dosed daily for 10 days. **C,** Average number of functional microvessels ($CD31^+$/*Le*-$Lectin^+$) in tumors of mice dosed daily at 80 mg/kg/day for up to 10 days. **D,** Average fraction of functional microvessels ($CD31^+$/*Le*-$Lectin^+$) *vs.* total tumor microvessels ($CD31^+$) in tumors of mice dosed daily at 80 mg/kg/day for up to 10 days. Statistical analysis was by one-way ANOVA (post hoc by Dunnett's multiple comparisons test:
* $P < 0.05$; ** $P < 0.01$; *** $P < 0.001$).

Figure S6. sHHI modulation of tumor IFP: effect of higher dose

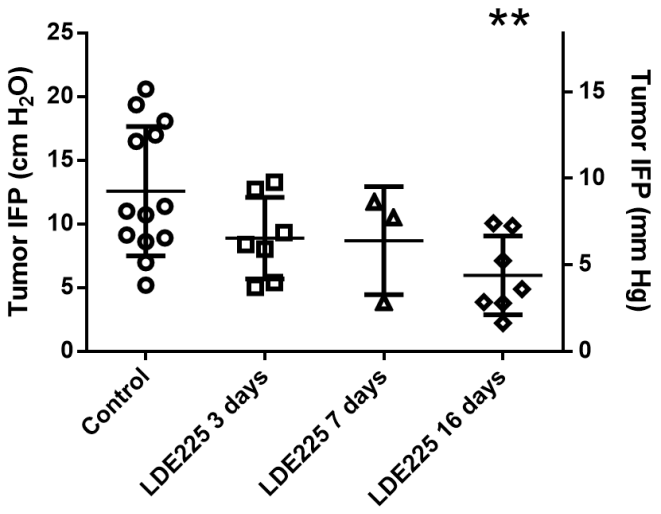

Mice bearing PDX #18269 tumors were was dosed daily *p.o.* with NVP-LDE225 (80 mg/kg/day) for up to 16 days. Tumor IFP was measured by inserting a 23½ gauge needle catheter that was hydraulically-coupled to a pressure transducer to increasing depths within the tumor. The maximum stable pressure is reported. Each data point represents one animal. Statistical analysis: t test with Welch's correction; ** $P \leq 0.01$.

Figure S7. Total and phosphorylated EGFR in PDX #18269

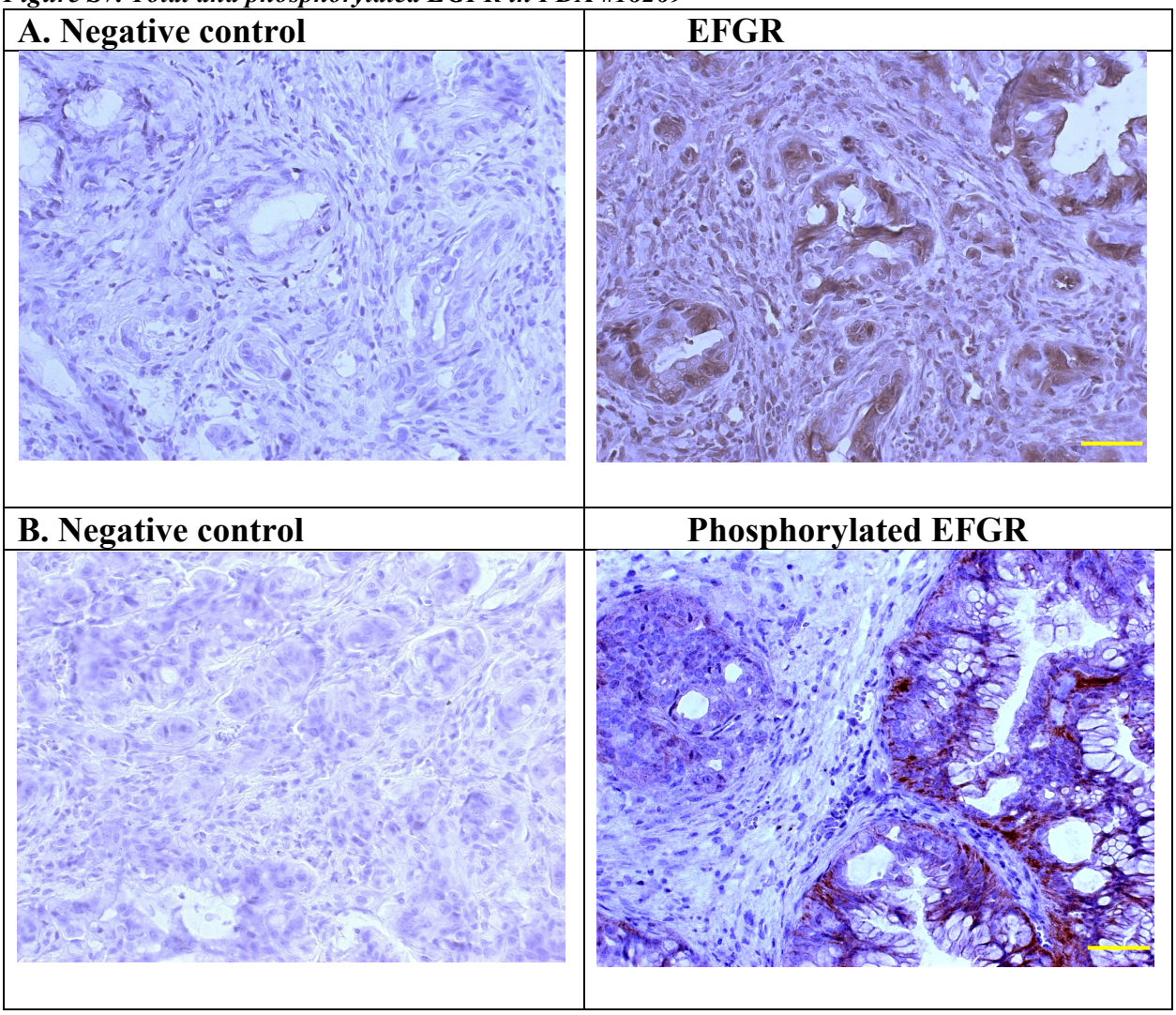

Total- and phosphorylated EGFR were probed in PDX #18269 tumors by immunohistochemistry as described in the parent manuscript. Primary antibodies were anti-EGFR (ab2430, Abcam, Cambridge MA) and anti-pEGFR (#2235, Cell Signaling Technology, Danvers, MA) (5). Positive cells are indicated by the brown reaction product that is confined to the adenocarcinoma cells.
A, Total EGFR. Left panel: negative control (no primary antibody). Right panel: EGFR staining.
B, Phosphorylated EGFR. Left panel: negative control (no primary antibody). Right panel: p-EGFR staining. Scale bar: 50 um.
C. Total- and phosphorylated EGFR expression in cultured pancreatic cancer cell line samples (Mia PaCA-2, Panc-1) and PDAC PDX tumors #14312 and #18269. Approx. 20 μg protein was loaded in each lane, except for those marked '5x' and '10x', which were loaded with 100 and 500 μg, respectively, to compensate for the low abundance of tumor cells in these stroma-rich tumors. Whereas the cell line samples were negative for pEGFR, the #18269 tumor, when loaded with the same approximate total EGFR protein, appeared weakly positive for pEGFR.

Figure S8. Distribution of tumor-targeted- vs non-targeted mAbs in tumors

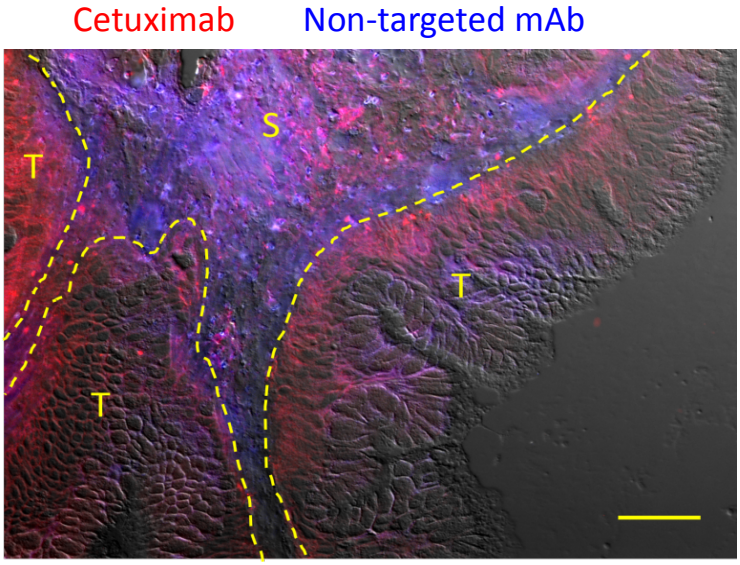

Mice bearing tumor #18269 were treated daily *p.o.* with sHHI (40 mg/kg/day), and after 7 days of treatment were injected *i.v.* with a mixture of two monoclonal antibodies (mAb): cetuximab (7.0 mg/kg) labeled with AlexaFluor 647 (ThermoFisher, Waltham, MA) and 8C2, a non-targeted (anti-topotecan) mAb (3.9 mg/kg) labeled with AlexaFluor 350. Mice were sacrificed at intervals to evaluate the amount of mAb deposition and its intra-tumor distribution. Five random sections from each of 3 mice/time point were imaged under identical acquisition conditions using wavelengths appropriate for the fluorophores. A Differential Interference Contrast (DIC) image was also acquired to permit image segmentation into stromal (S) and tumor cell (T) regions. The image shown was obtained 12 hours after administration of the mAbs. Red: AlexaFluor 647-labeled cetuximab; blue: AlexaFluor 350-labeled non-targeted mAb 8C2. Overlay: DIC image used for image segmentation. Scale bar: 50 µm.

Figure S9. Treatment regimen for antitumor efficacy experiments

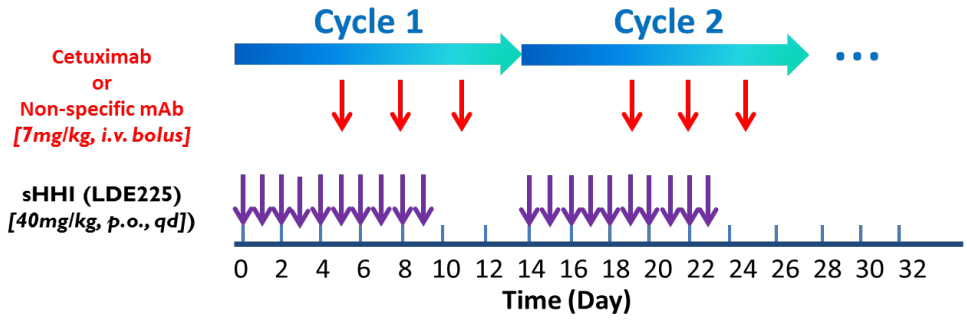

Each treatment cycle was 14 days. The sHHI was administered at 40 mg/kg/day *p.o.* for 10 days (purple arrows) and then withdrawn for 4 days. Cetuximab (7.0 mg/kg) or a non-targeted mAb (rituximab; 7.0 mg/kg) was administered *i.v.* on days 5, 8, and 11 (red arrows). The 14-day treatment cycles were repeated 6 times. Each treatment group had seven mice.

Figure S10. Plasma pharmacokinetics of cetuximab

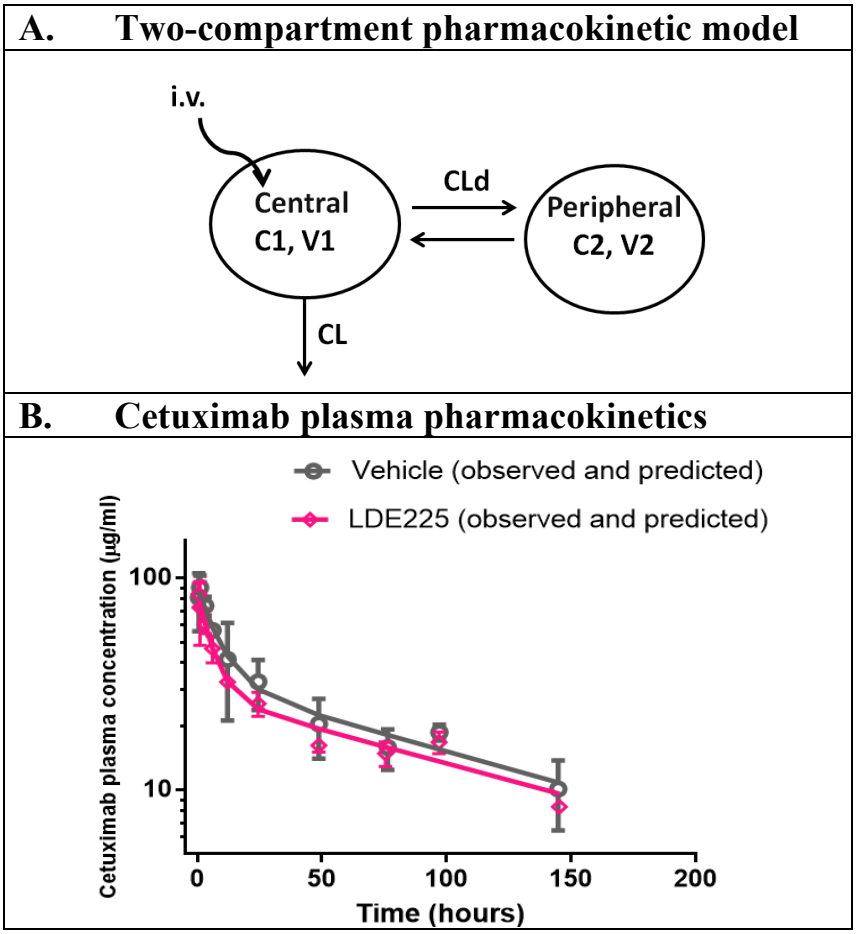

A, Structure of model for cetuximab plasma pharmacokinetics (PK) after *i.v.* administration. C1, plasma concentration; C2, concentration in the hypothetical peripheral compartment; V1, apparent volume of the central compartment; V2, apparent volume of peripheral compartment; CL, systemic clearance; CLd, distributional clearance; *i.v.*, intravenous input of cetuximab. **B,** Observed and model-predicted cetuximab plasma concentrations. A single bolus of cetuximab (7.0 mg/kg) labeled with AlexaFluor 647 was administered *i.v.* to mice bearing PDX tumor #18269 that were pre-dosed with sHHI (40 mg/kg/day *p.o.*) for 7 days before cetuximab administration. The sHHI dosing continued through the end of the experiment. Control mice received vehicle without sHHI. Symbols represent the mean of 3 animals per time point with the standard deviation shown. Lines represent model fitting of the data. Figure 6 of the parent publication shows estimated cetuximab plasma concentrations for the multiple-dose treatment regimen.

Figure S11. Effect of sHHI/antibody treatment regimen on tumor volume progression in individual mice

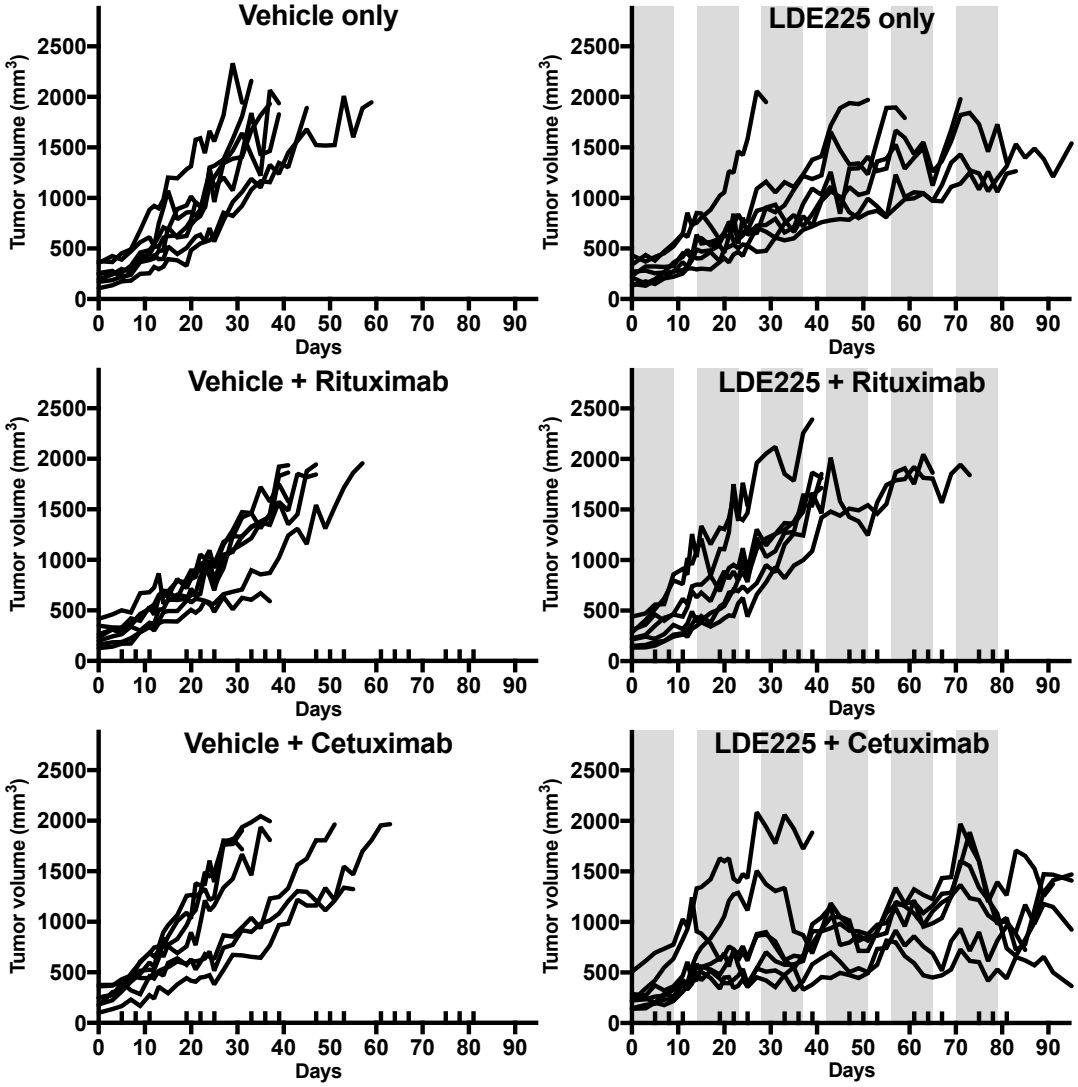

Tumor volume progression of PDX tumor #18269 for each of n=7 mice allocated to treatment groups as indicated by the title in each panel. Experiment consisted of 6 treatment cycles of 10 days with sHHI administered *p.o.* daily (vertical grey bands; NVP-LDE225 at 40 mg/kg/day) and mAb was administered *i.v.* on day 5, 8, and 11 (vertical ticks on abscissa; 7 mg/kg/dose). The inter-cycle interval between sHHI treatments was 4 days.

References

1. Roy Chaudhuri T, Straubinger NL, Pitoniak RF, Hylander BL, Repasky EA, Ma WW, et al. Tumor-priming Smoothened inhibitor enhances deposition and efficacy of cytotoxic nanoparticles in a pancreatic cancer model. Mol Cancer Ther 2016;15:84-93.
2. Meers P, Ali S, Erukulla R, Janoff AS. Novel inner monolayer fusion assays reveal differential monolayer mixing associated with cation-dependent membrane fusion. Biochim Biophys Acta 2000;1467:227-43.
3. Saito R, Bringas JR, McKnight TR, Wendland MF, Mamot C, Drummond DC, et al. Distribution of liposomes into brain and rat brain tumor models by convection-enhanced delivery monitored with magnetic resonance imaging. Cancer Res 2004;64:2572-9.
4. Hylander BL, Pitoniak R, Penetrante RB, Gibbs JF, Oktay D, Cheng J, et al. The anti-tumor effect of Apo2L/TRAIL on patient pancreatic adenocarcinomas grown as xenografts in SCID mice. J Transl Med 2005;3:22-35.
5. Tsakiridis T, Cutz JC, Singh G, Hirte H, Okawara G, Corbett T, et al. Association of phosphorylated epidermal growth factor receptor with survival in patients with locally advanced non-small cell lung cancer treated with radiotherapy. J Thorac Oncol 2008;3:716-22.